

A density functional study of $[M(\text{PH}_3)_2(\eta^2\text{-C}_2\text{X}_4)]$ alkene complexes for the Group 10 metals Ni, Pd, Pt: the effect of electron-attracting substituents

Francesco Nunzi,^a Antonio Sgamellotti,^{*a} Nazzareno Re^b and Carlo Floriani^c

^a Dipartimento di Chimica e Centro Studi CNR per il Calcolo Intensivo in Scienze Molecolari, Università di Perugia, I-06123 Perugia, Italy

^b Facoltà di Farmacia, Università G. D'Annunzio, I-66100 Chieti, Italy

^c Institut de Chimie Minérale et Analytique, Université de Lausanne, CH-1015 Lausanne, Switzerland

Received 15th June 1999, Accepted 20th July 1999

Density functional calculations have been performed for $[M(\text{PH}_3)_2(\text{C}_2\text{X}_4)]$ complexes with $M = \text{Ni, Pd or Pt}$ and $X = \text{H, F or CN}$ to study the effect of electron-attracting substituents on the metal–olefin bonding. The optimised geometries have been found to be in good agreement with experimental crystal structure data. The electronic structure has been analysed in terms of the Chatt–Dewar–Duncanson model and the contribution from π back donation was found to dominate over that from σ donation for both ethylene and substituted ethylene complexes. Reliable values have been calculated for the metal–olefin bond dissociation energies and compared with the available experimental data.

1 Introduction

Low-valent ML_2 complexes of the nickel triad with olefins are a well studied class of compounds.^{1–4} In particular, several $[M(\text{PR}_3)_2(\text{olefin})]$ complexes have been structurally characterised and spectroscopically investigated.² Despite the vast literature on these metal olefin complexes, there are still important gaps in some experimental information. First, no such palladium complex has been structurally characterised by X-ray crystallography, probably because of the labile palladium–olefin bond. Secondly, the thermodynamic data on the metal–olefin bond strength are sparse and limited to a few systems.⁵ Finally, very few experimental data are available for the complexes of electron-deficient substituted olefins.^{3,4}

The recent investigations on transition metal fullerene complexes⁶ pointed out their similarity to the metal complexes of electron-deficient olefins, in particular to fluoro and cyano substituted ethylene. It would therefore be useful to investigate the latter complexes and to provide computationally derived estimates of their main structural and energetic parameters.

Several theoretical calculations have been performed on transition metal complexes of ethylene,⁷ but most at the non-correlated level and cover only unsubstituted ethylene. Recently, metal diphosphine complexes of ethylene have been studied theoretically by Ziegler and co-workers,^{7e} using a density functional non-local approach within a more general study of the influence of relativistic effects on the metal–ligand bond in several π complexes.

In this work we carry out an accurate theoretical study on the $[M(\text{PH}_3)_2(\text{C}_2\text{X}_4)]$ substituted ethylene complexes ($X = \text{H, F or CN}$) for the Group 10 metals Ni, Pd, Pt at the DFT non-local level. The aim of this study is to investigate the electronic structure of these complexes, with special attention paid to the relative importance of σ donation and π back donation, and its dependence on the olefin substituents. We will also give reliable theoretical estimates for the bond dissociation energies of the considered complexes and discuss critically the available experimental data.

2 Computational details

The calculations reported are based on the ADF (Amsterdam Density Functional) program package.⁸ Its main characteristics are the use of a density fitting procedure to obtain accurate Coulomb and exchange potentials in each SCF cycle, the accurate and efficient numerical integration of the effective one-electron Hamiltonian matrix elements and the possibility to freeze core orbitals. The molecular orbitals were expanded in an uncontracted triple- ζ Slater-type orbitals (STO) basis set for all main group atoms. For transition metal orbitals we used a double- ζ STO basis set for ns and np and a triple- ζ STO basis set for nd and $(n + 1)s$. As polarisation functions, we used one $(n + 1)p$ function for transition metals, one $3d$ for P, C, N and F, and one $2p$ for H. The inner shell cores have been kept frozen.

The local density approximation (LDA) exchange correlation potential and energy were used, together with the Vosko–Wilk–Nusair parametrisation⁹ for homogeneous electron gas correlation, including Becke's non-local correction¹⁰ to the local exchange expression and Perdew's non-local correction¹¹ to the local expression of correlation energy. Molecular structures of all considered complexes were optimised at this non-local (NL) level in C_{2v} symmetry.

3 Results and discussion

Geometry optimisation

All crystal structures available for metal diphosphine ethylene complexes show the C–C bond in the MP_2 plane (**A** in Fig. 1) rather than perpendicular to it (**B**). All geometry optimisations on ethylene complexes were therefore performed in the parallel orientation **A** with imposed C_{2v} symmetry constraints. The preference for the parallel orientation has been checked in the $[\text{Pt}(\text{PH}_3)_2(\text{C}_2\text{H}_4)]$ complex for which the perpendicular structure (optimised with C_{2v} symmetry constraints) has been found 149 kJ mol^{-1} higher than the parallel one in agreement with the

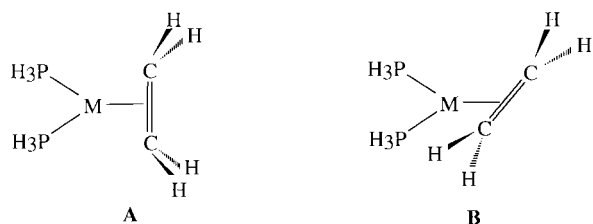


Fig. 1 Parallel (A) and perpendicular (B) orientations of ethylene complexes.

experimental evidence. Indeed, the ^{13}C NMR spectrum of $[\text{Pt}(\text{PPh}_3)_2(\text{C}_2\text{H}_4)]$ showed an AX Y pattern (due to the coupling with the two ^{31}P nuclei) up to the decomposition temperature of 70 °C, indicating a barrier to internal rotation higher than 80 kJ mol $^{-1}$.¹²

The results of the geometry optimisation for all considered $[\text{M}(\text{PH}_3)_2(\text{C}_2\text{X}_4)]$ complexes show a significant distortion of the olefin with a lengthening of the C–C bond and a significant deviation from planarity. The distortion from planarity is indicated by the pyramidalisation angle, defined as the angle between the C–C axis and the plane containing one of these carbon atoms and its two neighbouring atoms X.

The computed parameters are reported in Tables 1–3, respectively for X = H, F, or CN, and compared with the available experimental values. A direct comparison between theoretical and experimental geometries is difficult as most of the observed structures refer to aryl or alkyl substituted phosphines and multiply substituted olefins. In particular, the experimental data in Tables 1–3 refer to $[\text{Ni}(\text{PPh}_3)_2(\text{C}_2\text{H}_4)]$,¹⁴ $[\text{Pt}(\text{PPh}_3)_2(\text{C}_2\text{H}_4)]$,¹³ $[\text{Pt}(\text{PPh}_3)_2\{\text{C}_2\text{F}_2(\text{CF}_3)_2\}]$ ³ and $[\text{Pt}(\text{PPh}_3)_2\{\text{C}_2(\text{CN})_4\}]$.⁴ The calculated values compare quite well with the available experimental data. Bond length deviations are within only 0.04 Å and could, in part, be due to the use of model PH_3 ligands on the metal atoms which are less electron releasing than the PPh_3 or PEt_3 ligands on the actual complexes. In fact, a recent theoretical study has shown that the use of PH_3 ligand in place of aryl or alkyl substituted phosphines could lead to significant differences in the geometrical structure of the corresponding complexes.¹⁵

It is noteworthy that the computed M–P bond lengths reproduce fairly well the experimental data for Ni and Pt. The description of the metal–phosphorus bond is quite difficult and previous *ab initio* calculations at Hartree–Fock (HF) level on $[\text{Pt}(\text{PH}_3)_2(\text{C}_2\text{H}_4)]$ led to remarkable deviations of the Pt–P bond length from the experimental value. A deviation of 0.17 Å was calculated by Morokuma and Borden^{7f} at HF level using a relativistic electron core potential (ECP) with a double- ζ valence basis set for Pt and a double- ζ basis set for all other atoms. The inclusion of polarisation functions and correlation through the DFT NL approach leads to an excellent agreement of the computed Pt–P bond length with the experimental values, the deviation being within only 0.01 Å.

According to the above results, the distortion of the coordinated olefin is smaller in the palladium ethylene complexes than in the corresponding nickel and platinum complexes. This result cannot be compared with any experimental data, since, to our knowledge, no palladium complex has been structurally characterised. However, such a result is in accord with thermochemical experimental evidence indicating that the palladium olefin complexes are more labile than those of nickel and platinum.

The degree of distortion of ethylene upon co-ordination increases with substitution by electron-attracting groups F and CN. The lengthening of the C–C bond, which is 0.06–0.11 Å for ethylene, increases to 0.09–0.19 Å for tetrafluoro- and tetracyano-ethylene (see Tables 1–3). Note that the C–C bond distance in tetracyanoethylene coordinated to platinum (1.516 Å) is close to that of C–C bonds in saturated hydrocarbons.

Table 1 Optimised geometries^a of $[\text{M}(\text{PH}_3)_2(\text{C}_2\text{H}_4)]$ complexes

Molecule	$R_{(\text{C}-\text{C})}$	$R_{(\text{M}-\text{C})}$	$R_{(\text{M}-\text{P})}$	P–M–P	δ
Calculated					
$[\text{Ni}(\text{PH}_3)_2(\text{C}_2\text{H}_4)]$	1.404	2.032	2.184	112.0	18.6
$[\text{Pd}(\text{PH}_3)_2(\text{C}_2\text{H}_4)]$	1.393	2.242	2.359	111.4	16.0
$[\text{Pt}(\text{PH}_3)_2(\text{C}_2\text{H}_4)]$	1.443	2.097	2.259	107.2	27.0
Experimental					
$[\text{Ni}(\text{PPh}_3)_2(\text{C}_2\text{H}_4)]^b$	1.430	1.990	2.152	110.5	—
$[\text{Pt}(\text{PPh}_3)_2(\text{C}_2\text{H}_4)]^c$	1.434	2.112	2.268	111.6	—

^a Bond lengths in angstroms and bond angles in degrees. ^b Ref. 14. ^c Ref. 13.

Table 2 Optimised geometries^a of $[\text{M}(\text{PH}_3)_2(\text{C}_2\text{F}_4)]$ complexes

Molecule	$R_{(\text{C}-\text{C})}$	$R_{(\text{M}-\text{C})}$	$R_{(\text{M}-\text{P})}$	P–M–P	δ
Calculated					
$[\text{Ni}(\text{PH}_3)_2(\text{C}_2\text{F}_4)]$	1.422	1.948	2.221	109.7	32.5
$[\text{Pd}(\text{PH}_3)_2(\text{C}_2\text{F}_4)]$	1.422	2.128	2.393	108.9	31.9
$[\text{Pt}(\text{PH}_3)_2(\text{C}_2\text{F}_4)]$	1.468	2.043	2.304	104.8	36.3
Experimental					
$[\text{Pt}(\text{PPh}_3)_2\{\text{C}_2\text{F}_2(\text{CF}_3)_2\}]^b$	1.429	2.038	2.312	105.9	—

^a Bond lengths in angstroms and bond angles in degrees. ^b Ref. 3.

Table 3 Optimised geometries^a of $[\text{M}(\text{PH}_3)_2\{\text{C}_2(\text{CN})_4\}]$ complexes

Molecule	$R_{(\text{C}-\text{C})}$	$R_{(\text{M}-\text{C})}$	$R_{(\text{M}-\text{P})}$	P–M–P	δ
Calculated					
$[\text{Ni}(\text{PH}_3)_2\{\text{C}_2(\text{CN})_4\}]$	1.473	1.998	2.234	105.5	19.5
$[\text{Pd}(\text{PH}_3)_2\{\text{C}_2(\text{CN})_4\}]$	1.468	2.178	2.384	105.9	19.5
$[\text{Pt}(\text{PH}_3)_2\{\text{C}_2(\text{CN})_4\}]$	1.516	2.102	2.283	103.2	27.2
Experimental					
$[\text{Pt}(\text{PPh}_3)_2\{\text{C}_2(\text{CN})_4\}]^b$	1.49	2.11	2.289	101.4	—

^a Bond lengths in angstroms and bond angles in degrees. ^b Ref. 4.

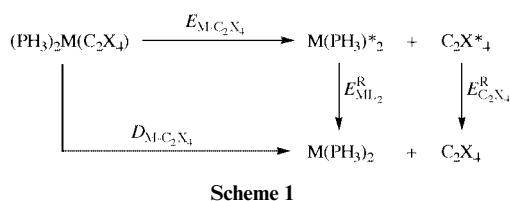
Also the pyramidalisation angle, δ , calculated to be about 16–27° for $[\text{M}(\text{PH}_3)_2(\text{C}_2\text{H}_4)]$, increases to 20–36° for substituted olefin complexes. The C_2F_4 and $\text{C}_2(\text{CN})_4$ complexes have quite similar C–C bond lengthening, however $\text{C}_2(\text{CN})_4$ complexes have pyramidalisation angles 10° smaller with respect to C_2F_4 complexes. The minor deviation from planarity of $\text{C}_2(\text{CN})_4$ is probably due to the conjugation between the CN triple bond and CC double bond.

Bonding energies

The bond dissociation energies between the C_2X_4 and $\text{M}(\text{PH}_3)_2$ fragments, $D(\text{M}-\text{C}_2\text{X}_4)$, have been calculated according to eqn. (1) where both the olefin complex and the two fragments

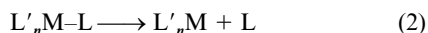


have been considered in their ground-state equilibrium geometries. Using the fragment-oriented approach of the DFT computational scheme implemented in the ADF program, the above bond dissociation energies are computed in two steps, as shown in Scheme 1. First we calculate the “snapping energies”,



$E^*(\text{M}-\text{C}_2\text{X}_4)$, *i.e.* the energies gained when snapping the metal–olefin bond, obtained by building $[\text{M}(\text{PH}_3)_2(\text{C}_2\text{X}_4)]$ from the fragments with the conformation they assume in the equilibrium geometry of the overall complex. In a second step we compute the energies $E_{\text{C}_2\text{X}_4}^R$ and $E_{\text{M}(\text{PH}_3)_2}^R$ gained when the isolated fragments relax to their equilibrium geometries. This approach also allows direct computation of the basis set superposition error (BSSE) by applying the counterpoise method.¹⁶ Corrections for the zero-point vibrations were not included since they are expected to be quite small. Indeed, the vibrational zero-point corrections to metal–ligand bonding energy have been estimated to be very small, less than 2 kJ mol⁻¹,¹⁷ for carbonyl which shows π -acceptor properties similar to those of substituted alkenes. A recent investigation of the effects of the basis set incompleteness on the bond dissociation energies of some metal–ligand and metal–metal bonds has led to the conclusion that triple- ζ plus polarisation basis sets give reasonably accurate bond energies for organometallic systems with sufficiently small BSSE corrections to warrant its neglect in most situations.¹⁸

The above computational scheme is particularly convenient as it parallels the most recent convention used to discuss thermochemical data in terms of the two parameters usually considered to measure metal–ligand “bond strengths”.⁵ According to this convention, reviewed by Simões and Beauchamp,^{5c} the bond dissociation enthalpy, $D(\text{M}-\text{L})$ is defined as the enthalpy change of the ligand dissociation process, eqn. (2), and is composed of contributions from an

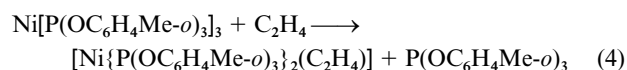


“intrinsic” bond enthalpy term $E(\text{M}-\text{L})$, the energy required to snap the $\text{M}-\text{L}$ bond into non-reorganised fragments, and the fragment reorganisation energies $E_R(\text{M})$ and $E_R(\text{L})$. Therefore, if we neglect the small thermal correction to enthalpy, we can identify the bond dissociation enthalpy with the calculated bond dissociation energy and the bond enthalpy term with the calculated snapping energies corrected by BSSE.

The results obtained are given in Table 4, where we report all the various contributions, *i.e.* snapping energies, relaxation energies and BSSEs. Table 4 shows that the metal–ethylene bond dissociation energies increase in the order Pd < Pt < Ni in agreement with the observed stability order deduced from experimental equilibrium constants for reaction (3).^{5a} The value



calculated for Ni, 123 kJ mol⁻¹, compares quite well with the available experimental data of 138 kJ mol⁻¹ evaluated for reaction (4) from equilibrium studies in solution on the assump-



tions that the solvation enthalpies of $\text{Ni}[\text{P}(\text{OC}_6\text{H}_4\text{Me-}o)_3]_3$ and $[\text{Ni}\{\text{P}(\text{OC}_6\text{H}_4\text{Me-}o)_3\}_2(\text{C}_2\text{H}_4)]$ cancel, and that the value of $D(\text{Ni}-\text{P})$ in $\text{Ni}[\text{P}(\text{OC}_6\text{H}_4\text{Me-}o)_3]_3$ is the same as that observed for $\text{Ni}[\text{P}(\text{OC}_6\text{H}_4\text{Me-}o)_3]_4$.¹⁹

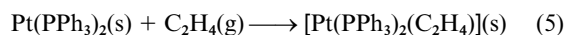
Experimental values are available for Pt–C₂H₄ bond dissociation energy derived from (i) solution microcalorimetry data on

Table 4 Calculated bond dissociation energies (kJ mol⁻¹) for the $[\text{M}(\text{PH}_3)_2(\text{C}_2\text{X}_4)]$ complexes

Complex	E^*	BSSE	E^a	$E_{\text{M}(\text{PH}_3)_2}^R$	$E_{\text{C}_2\text{X}_4}^R$	D_e
$[\text{Ni}(\text{PH}_3)_2(\text{C}_2\text{H}_4)]$	194	5	189	37	30	123
$[\text{Pd}(\text{PH}_3)_2(\text{C}_2\text{H}_4)]$	121	2	118	39	21	58
$[\text{Pt}(\text{PH}_3)_2(\text{C}_2\text{H}_4)]$	308	3	304	141	61	102
$[\text{Ni}(\text{PH}_3)_2(\text{C}_2\text{F}_4)]$	295	12	283	48	110	125
$[\text{Pd}(\text{PH}_3)_2(\text{C}_2\text{F}_4)]$	205	11	194	48	105	41
$[\text{Pt}(\text{PH}_3)_2(\text{C}_2\text{F}_4)]$	434	12	422	158	101	163
$[\text{Ni}(\text{PH}_3)_2\{\text{C}_2(\text{CN})_4\}]$	297	11	285	57	40	188
$[\text{Pd}(\text{PH}_3)_2\{\text{C}_2(\text{CN})_4\}]$	206	8	199	54	38	106
$[\text{Pt}(\text{PH}_3)_2\{\text{C}_2(\text{CN})_4\}]$	372	8	364	159	77	128

^a $E = E^* + \text{BSSE}$.

the enthalpy of formation for $[\text{Pt}(\text{PPh}_3)_2(\text{C}_2\text{H}_4)]$ and $[\text{Pt}(\text{PPh}_3)_2\text{Cl}_2]$,²⁰ and (ii) direct calorimetry measurements for the heterogeneous phase reaction (5).²¹ The former study relies on



the assumptions of a negligible reorganisation energy associated with the $(\text{PPh}_3)_2\text{Pt}$ fragment and a value of 290 kJ mol⁻¹ for the Pt–Cl bond energy term, and gave a value of 152 kJ mol⁻¹ for $D(\text{Pt}-\text{C}_2\text{H}_4)$. However, such a value is larger than the estimate of 138 kJ mol⁻¹ for the bond dissociation enthalpy in $[\text{Ni}\{\text{P}(\text{OC}_6\text{H}_4\text{Me-}o)_3\}_2(\text{C}_2\text{H}_4)]$ and disagrees with the experimental evidence that the stability of metal–ethylene bonds does increase in the order Pd < Pt < Ni (see above).^{5a} A value significantly lower than 152 kJ mol⁻¹ therefore seems more consistent with the latter reliable experimental data^{5a} on the relative equilibrium constants for complexes of Ni, Pd and Pt, and would compare reasonably with our calculated value of 102 kJ mol⁻¹.

The reorganisation energy calculated for the $(\text{PH}_3)_2\text{Pt}$ fragment, 141 kJ mol⁻¹, points out possible reasons for the overestimate of the experimental data of ref. 20. In fact, the latter data rely on the assumption that the reorganisation energy of the $(\text{PPh}_3)_2\text{Pt}$ fragment from the geometry it has in the $[\text{Pt}(\text{PPh}_3)_2(\text{C}_2\text{H}_4)]$ complex to that in $[\text{Pt}(\text{PPh}_3)_2\text{Cl}_2]$ is negligible. However, this energy contribution could be a significant part of the whole reorganisation energy of the $(\text{PPh}_3)_2\text{Pt}$ fragment to the optimised linear structure (141 kJ mol⁻¹) and therefore of the order of 50 kJ mol⁻¹.

To our knowledge there are only three previous correlated calculations of the bond dissociation energy for $[\text{Pt}(\text{PH}_3)_2(\text{C}_2\text{H}_4)]$. Sakaki and Ieki^{7h} performed MP4 calculations on a HF optimised geometry, obtaining 85 kJ mol⁻¹ while Ziegler and co-workers^{7e} carried out DFT NL calculations, obtaining 95 kJ mol⁻¹. A more recent calculation by Frenking *et al.*²² at the CCSD(T)//MP2 level of theory gave a value of 118 kJ mol⁻¹ in good agreement with our results.

The inaccuracy of the experimental data available for $D(\text{Pt}-\text{C}_2\text{H}_4)$ is supported by the discordant results of a different thermochemical study.²¹ Indeed, the direct calorimetric study of ref. 21 gave a value of 12 kJ mol⁻¹ for the heat of ethylene addition to bis(triphenylphosphine)platinum, reaction (5), which would provide a rough approximation to $D(\text{Pt}-\text{C}_2\text{H}_4)$ on the assumption that the sublimation energies of $(\text{PPh}_3)_2\text{Pt}$ and $[\text{Pt}(\text{PPh}_3)_2(\text{C}_2\text{H}_4)]$ cancel. This value seems to be a severe underestimate, probably because the sublimation energy for the more symmetric $(\text{PPh}_3)_2\text{Pt}$ species is significantly higher than that for the corresponding ethylene complex. However, the sublimation energy difference could hardly be higher than 50–80 kJ mol⁻¹ leading to a value of $D(\text{Pt}-\text{C}_2\text{H}_4)$ smaller than 100 kJ mol⁻¹, thus confirming our suggestions that the value of 152 kJ mol⁻¹ of ref. 20 is overestimated by at least 50 kJ mol⁻¹.

Our results indicate the difficulties that arise when bond dissociation enthalpies are derived from thermochemical data on the basis of uncritical assumptions, especially in the presence of

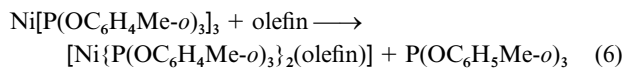
reorganisation energies, and the important role that accurate theoretical calculations can play in these situations.

The reorganisation energies calculated for the platinum diphosphine fragment (see Table 4) also explain the dichotomy presented by the thermodynamical and structural data on the metal–ethylene bond strength within the nickel triad. Thermochemical information derived from equilibrium constant measurements^{5a} indicates that the metal–ethylene bond dissociation energies increase in the order Pd < Pt < Ni, while structural data on nickel¹³ and platinum¹⁴ ethylene complexes indicate clearly a higher degree of distortion of the co-ordinated olefin in the platinum complexes thus suggesting a reversed bond strength order, *i.e.* Ni < Pt. Table 4 shows that the order of the metal–ethylene bond dissociation energies for the two latter metals (102 and 123 kJ mol⁻¹, respectively for Pt and Ni) is determined by the reorganisation energy of the (PH₃)₂Pt fragment while the order of the bond energy terms is reversed (304 and 189 kJ mol⁻¹, respectively for Pt and Ni). On the other hand, the bond enthalpy term seems to be the right thermodynamic parameter to correlate with structural and spectroscopic data, such as bond lengths, angles, solid cone angles and force constants.^{5c}

The above discussion illustrates that the use of structural data to infer trends regarding thermodynamics can be misleading and provides an example of the necessary considerations that must be given to reorganisation energies when evaluating metal–ligand bond strength. Theoretical calculations can be very useful, allowing the evaluation of the experimentally inaccessible fragment reorganisation energies.

The comparison between the calculated thermodynamic parameters for ethylene complexes and those for fluoro and cyano substituted ethylene complexes (see Table 4) shows that the bond energy terms for the C₂F₄ and C₂(CN)₄ complexes are *ca.* 60–120 kJ mol⁻¹ higher. This result agrees with the experimental evidence showing for the co-ordinated tetrafluoro- and tetracyano-ethylene a longer C–C bond length and a larger pyramidalisation angle (see Tables 1–3) than for ethylene. A less clear trend is observed for the bond dissociation energies, due to the different reorganisation energies of the tetrafluoro- and tetracyano-ethylene fragments. There is an evident increase of 40–60 kJ mol⁻¹ from ethylene to tetracyanoethylene complexes; on the other hand passing on from ethylene to tetrafluoroethylene the bond dissociation energies remain essentially constant or slightly decrease for Ni and Pd, but increase for Pt.

Few and sparse thermochemical data are available for the fluoro and cyano substituted olefin complexes of the nickel triad, making direct comparison of the calculated and experimental bond dissociation enthalpies a difficult task. Equilibrium studies in solution of reaction (6) conducted on several



substituted ethylenes¹⁹ gave an estimate of 176 kJ mol⁻¹ for the *trans*-dicyanoethylene which compares reasonably with our calculated value of 188 kJ mol⁻¹ for the tetracyanoethylene nickel complex. The same study¹⁹ also gave for the tetrafluoroethylene complex of nickel a stability constant close to that for ethylene and then essentially the same bond dissociation enthalpy, in agreement with our calculations (123 and 125 kJ mol⁻¹ respectively for C₂H₄ and C₂F₄). Solution microcalorimetry data on the enthalpy of formation for [Pt(PPh₃)₂(C₂H₄)] and [Pt(PPh₃)₂Cl₂]²⁰ led to a value of 277 kJ mol⁻¹ for *D*(Pt–C₂(CN)₄). This experimental dissociation energy is much larger than the calculated value of 128 kJ mol⁻¹, a disagreement analogous to that also observed for ethylene. This could again be attributed to the overestimate of the experimental data in ref. 20, probably due to the unjustified assumptions on which the experimental data rely (see the discussion above for the platinum ethylene complex). Note, however, that the increase of bond dissociation

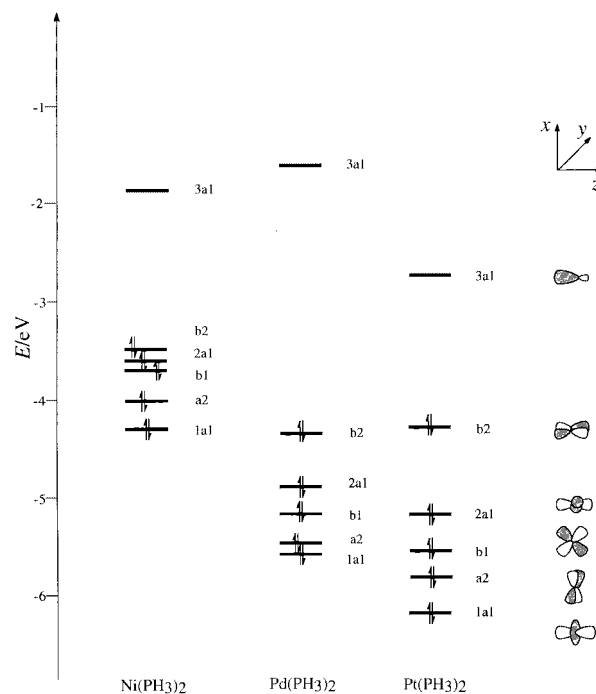


Fig. 2 Main valence orbitals of M(PH₃)₂ metal fragments.

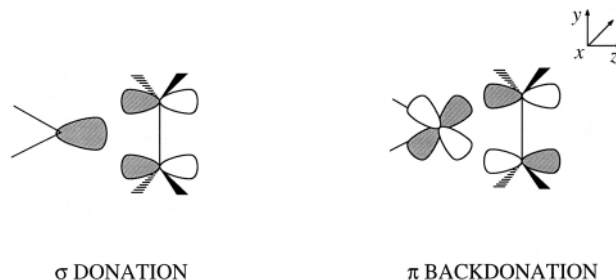


Fig. 3 Orbital interactions in the Dewar–Chatt–Duncanson model.

energy experimentally observed on passing from ethylene to tetracyanoethylene complexes (from 152 to 277 kJ mol⁻¹) is reproduced by our calculations (from 102 to 128 kJ mol⁻¹).

Analysis of the electronic structure

The bonding of a side-on co-ordinated π ligand to a transition metal fragment is usually described by the Dewar–Chatt–Duncanson model.²³ According to this model, the bonding arises from the electron donation from a filled π orbital of the ligand to a suitable vacant metal orbital (σ donation), and the simultaneous back donation from an occupied metal d orbital to the vacant π^* orbital of the ligand (π back donation). All three considered M(PH₃)₂ metal fragments show a LUMO of a₁ symmetry with hybrid s–p_z character, and two filled b₁ and b₂ orbitals of d_x character, see Fig. 2. The σ donation involves essentially the empty metal a₁ orbital and the filled π orbital of C₂X₄, while the π back donation involves the filled b₂(d_{yz}) metal orbital, lying in the MC₂ plane, and the empty π^* orbital of C₂X₄, see Fig. 3.

In order to separate the contributions from σ donation and π back donation we employed an analysis of the metal–olefin bond dissociation energies based on the extended transition state method.^{24a} The bond dissociation energy is decomposed into a number of contributions, eqn. (7). The first term, E_{prep} , is

$$D(\text{M}-\text{C}_2\text{X}_4) = -[E_{\text{prep}} + E_{\text{ster}} + E_{\text{orb}}] \quad (7)$$

the energy necessary to convert the fragments from their equilibrium geometries into the conformation they assume in the optimised structure of the overall complex. Since the fragments

Table 5 Bond dissociation energy decomposition (kJ mol⁻¹) for the [M(PH₃)₂(C₂X₄)] complexes

Complex	E_{ster}	E_{orb}	E_{A1}	E_{A2}	E_{B1}	E_{B2}
[Ni(PH ₃) ₂ (C ₂ H ₄)]	106	-300	-71	0	-13	-218
[Pd(PH ₃) ₂ (C ₂ H ₄)]	103	-224	-68	1	-10	-147
[Pt(PH ₃) ₂ (C ₂ H ₄)]	265	-529	-198	-3	-23	-301
[Ni(PH ₃) ₂ (C ₂ F ₄)]	187	-482	-74	-5	-51	-362
[Pd(PH ₃) ₂ (C ₂ F ₄)]	191	-396	-79	-5	-37	-285
[Pt(PH ₃) ₂ (C ₂ F ₄)]	315	-749	-214	-10	-62	-463
[Ni(PH ₃) ₂ {C ₂ (CN) ₄ }]	219	-515	-73	-8	-28	-418
[Pd(PH ₃) ₂ {C ₂ (CN) ₄ }]	210	-429	-71	-6	-23	-329
[Pt(PH ₃) ₂ {C ₂ (CN) ₄ }]	333	-705	-168	-10	-38	-502

have been considered in the same closed shell state both in the complex formation and as free molecules, this term corresponds simply to the sum of the fragment relaxation energies, $E^R_{C_2X_4} + E^R_{M(PH_3)_2}$. Here E_{ster} represents the steric repulsion between the two fragments and consists of two components. The first is the electrostatic interaction of the nuclear charges and the unmodified electronic charge density of one fragment with those of the other fragment. The second component is the so-called Pauli repulsion, which is essentially due to the anti-symmetry requirement on the total wavefunction. The orbital interaction term, E_{orb} , represents the attracting orbital interactions which give rise to the energy lowering upon coordination. This term may be broken up into contributions from the orbital interactions within the various irreducible representations Γ of the overall symmetry group of the system, according to the decomposition scheme proposed by Ziegler.^{24b}

This decomposition scheme is particularly useful in the considered complexes as it allows one to separate the energy contributions corresponding to σ donation (E_{A1}) and to π back donation (E_{B2}). Indeed, the ligand to metal donation takes place into the A_1 representation, while the metal to ligand back donation takes place into the B_2 representation. The results of this energy decomposition for all the considered olefin complexes are reported in Table 5. It follows from Table 5 that the contribution to the orbital interaction term from π back donation dominates over that from σ donation. It is worth noting that a recent charge density analysis (CDA) of metal–ethylene donor–acceptor interactions investigated at the MP2 level showed that ethylene is a stronger donor than acceptor in terms of charge transfer.²⁵ Therefore our results show that metal to ethylene π back donation, although implying a minor charge transfer, is energetically more important than ethylene to metal σ donation.

Table 5 also shows that most of the increase calculated for the bond energy terms on passing from ethylene to fluoro- and tetracyano-ethylene (80–120 kJ mol⁻¹) is due mainly the π back donation contribution, the σ contribution remaining almost constant. This can be explained by taking into account that C₂F₄ and C₂(CN)₄ have a higher electron affinity than ethylene, while the ionisation energies are comparable.

4 Conclusion

We have performed density functional calculations on the [M(PH₃)₂(η^2 -C₂X₄)] complexes for the Group 10 metals Ni, Pd, Pt at the DFT NL level. The optimised geometries have been found to be in good agreement with the X-ray experimental data. The electronic structure is analysed in terms of the Chatt–Dewar–Duncanson model and the contribution from π back donation dominates over that from σ donation for all complexes. Reliable values for the metal–olefin dissociation energies have been calculated. The bond dissociation energies calculated for the ethylene complexes increase in the order Pd < Pt < Ni in agreement with experimental evidence. Bond dissociation energies have been analysed in terms of “bond snapping energies” and fragment reorganisation energies, which allowed us to give a

rationale for the dichotomy between thermochemical and structural data on the metal–ethylene bond strength within the nickel triad. Fluoro- and cyano-substituted ethylene complexes show bond energy terms *ca.* 60–120 kJ mol⁻¹ higher than those calculated for the corresponding ethylene complexes while no clear trend is observed for the bond dissociation energies because of reorganisation energy effects.

Acknowledgements

The present work has been carried out in the context of the COST D9 Action. Foundation Herbette (University of Lausanne; to N. R.) is also acknowledged for financial support.

References

- 1 J. H. Nelson and H. B. Jonassen, *Coord. Chem. Rev.*, 1971, **6**, 27; S. D. Ittel and J. A. Ibers, *Adv. Organomet. Chem.*, 1976, **14**, 33; F. R. Hartley, in *Comprehensive Organometallic Chemistry*, ed. G. Wilkinson, Pergamon Press, Oxford, 1982, vol. 6.
- 2 C. C. Costain and B. P. Stoicheff, *J. Chem. Phys.*, 1959, **30**, 777; P. T. Cheng, C. D. Cook, C. H. Koo, S. C. Nyburg and M. T. Shiomu, *Acta Crystallogr., Sect. B*, 1971, **27**, 1904; P. W. Jolly, *The Organic Chemistry of Nickel*, Academic Press, New York, 1974, vol. 1.
- 3 J. M. Baraban and J. A. McKinney, *J. Am. Chem. Soc.*, 1975, **97**, 4232.
- 4 G. Bombieri, E. Forsellini, C. Panattoni, R. Graziani and G. Bandoli, *J. Chem. Soc. A*, 1970, 1313.
- 5 (a) F. R. Hartley, *Chem. Rev.*, 1973, **73**, 27; (b) *Comprehensive Organometallic Chemistry II*, eds. E. W. Abel, F. G. A. Stone and G. Wilkinson, Pergamon, Oxford, 1995, vol. 9, chs. 3, 6 and 9; (c) J. A. M. Simões and J. L. Beauchamp, *Chem. Rev.*, 1990, **90**, 629; (d) H. A. Skinner and J. A. Connor, *Pure Appl. Chem.*, 1985, **57**, 79.
- 6 P. J. Fagan, J. C. Calabrese and B. Malone, *Acc. Chem. Res.*, 1992, **25**, 390; A. H. H. Stephens and M. L. H. Green, *Adv. Inorg. Chem.*, 1997, **44**, 1; A. L. Balch and M. M. Olmstead, *Chem. Rev.*, 1998, **98**, 2123.
- 7 (a) P. J. Hay, *J. Am. Chem. Soc.*, 1981, **103**, 1390; (b) K. Kitaura, S. Sakaki and K. Morokuma, *Inorg. Chem.*, 1981, **20**, 2292; (c) T. Ziegler and A. Rauk, *Inorg. Chem.*, 1979, **18**, 1558; (d) T. Ziegler, *Inorg. Chem.*, 1985, **24**, 1547; (e) J. Li, G. Schreckenbach and T. Ziegler, *Inorg. Chem.*, 1995, **34**, 3245; (f) K. Morokuma and W. T. Borden, *J. Am. Chem. Soc.*, 1991, **113**, 1912; (g) S. Sakaki and K. Okubo, *J. Phys. Chem.*, 1989, **93**, 5655; (h) S. Sakaki and M. Ieki, *Inorg. Chem.*, 1991, **30**, 4218.
- 8 E. J. Baerends, D. E. Ellis and P. Ros, *Chem. Phys.*, 1973, **2**, 42; P. M. Boerrigter, G. te Velde and E. J. Baerends, *Int. J. Quantum Chem.*, 1988, **33**, 87.
- 9 S. H. Vosko, L. Wilk and M. Nusair, *Can. J. Phys.*, 1980, **58**, 1200.
- 10 A. D. Becke, *Phys. Rev. A*, 1988, **38**, 2398.
- 11 J. P. Perdew, *Phys. Rev. B*, 1986, **33**, 8822.
- 12 A. Kumar, J. D. Lichtenhan, S. C. Critchlow, B. E. Eichinger and W. T. Borden, *J. Am. Chem. Soc.*, 1990, **112**, 5633.
- 13 P. T. Cheng and S. C. Nyburg, *Can. J. Chem.*, 1972, **50**, 912.
- 14 L. J. Guggenberger, *Inorg. Chem.*, 1973, **12**, 499.
- 15 H. Jacobsen and H. Berke, *Chem. Eur. J.*, 1997, **3**, 881; O. Gonzales-Blanco and V. Branchadell, *Organometallics*, 1997, **16**, 5556.
- 16 S. F. Boys and F. Bernardi, *Mol. Phys.*, 1970, **19**, 553, *Organometallics*, 1997, **16**, 5556.
- 17 L. A. Barnes, M. Rosi and C. W. Bauschlicher, Jr., *J. Chem. Phys.*, 1991, **94**, 2031; L. A. Barnes, B. Liu and R. Lindth, *J. Chem. Phys.*, 1993, **98**, 3978.
- 18 A. Rosa, A. W. Ehlers, E. J. Baerends, J. G. Snijders and G. te Velde, *J. Phys. Chem.*, 1996, **100**, 5690.
- 19 C. A. Tolman, *J. Am. Chem. Soc.*, 1974, **96**, 2780.
- 20 G. Al Takhin, H. A. Skinner and A. A. Zaki, *J. Chem. Soc., Dalton Trans.*, 1984, 371; C. T. Mortimer, *Rev. Inorg. Chem.*, 1984, **6**, 233.
- 21 J. U. Mondial and D. M. Blake, *Coord. Chem. Rev.*, 1982, **47**, 205; W. G. Kirkham, M. W. Lister and R. B. Poyntz, *Thermochim. Acta*, 1975, **11**, 89.
- 22 G. Frenking, I. Antes, M. Böhme, S. Dapprich, A. W. Ehlers, V. Jonas, A. Neuhaus, M. Otto, R. Stegmann, A. Veldkamp and S. F. Vyboishchikov, *Rev. Comput. Chem.*, 1996, **8**, 63.
- 23 M. J. S. Dewar, *Bull. Soc. Chim. Fr.*, 1951, **18**, C71; J. Chatt and L. A. Duncanson, *J. Chem. Soc.*, 1953, 2939.
- 24 (a) T. Ziegler and A. Rauk, *Theor. Chim. Acta*, 1977, **46**, 1; (b) T. Ziegler, *NATO ASI Ser., Ser. C*, 1986, **176**, 189.
- 25 G. Frenking and U. Pidun, *J. Chem. Soc., Dalton Trans.*, 1997, 1653.